Inorg. Chem. **2002**, *41*, 3542–3547

Redox Energetics and Kinetics of Uranyl Coordination Complexes in Aqueous Solution

David E. Morris[†]

Chemistry Division and the G. T. Seaborg Institute for Transactinium Science, Los Alamos National Laboratory, Los Alamos, New Mexico 87545

Received March 4, 2002

Detailed voltammetric results for five uranyl coordination complexes are presented and analyzed using digital simulations of the voltammetric data to extract thermodynamic ($E_{1/2}$) and heterogeneous electron-transfer kinetic (k^0 and α) parameters for the one-electron reduction of UO_2^{2+} to UO_2^{+}. The complexes and their corresponding electrochemical parameters are the following: $[UO_2(OH_2)_5]^{2+}$ ($E_{1/2} = -0.169$ V vs Ag/AgCl, $k^0 = 9.0 \times 10^{-3}$ cm/s, and $\alpha = 0.50$); $[UO_2(OH)_5]^{3-}$ (–0.927 V, 2.8×10^{-3} cm/s, 0.46); $[UO_2(C_2H_3O_2)_3]^{-}$ (–0.396 V, ~0.1 cm/s, ~0.5); $[UO_2(CO_3)_3]^{4-}$ (–0.820 V, 2.6×10^{-5} cm/s, 0.41); $[UO_2Cl_4]^{2-}$ (–0.065 V, 9.2×10^{-3} cm/s, 0.30). Differences in the $E_{1/2}$ values are attributable principally to differences in the basicity of the equatorial ligands. Differences in rate constants are considered within the context of Marcus theory of electron transfer, but no specific structural change-(s) in the complexes between the two oxidation states can be uniquely identified with the underlying variability in the heterogeneous rate constants and electron-transfer coefficients.

Introduction

The redox chemistry of uranium is remarkably rich and diverse as a consequence of the number of readily accessible oxidation states (III−VI) and the sensitivity of the redox potentials to the coordination environment around the metal.[1−3] In aqueous environments, the most stable oxidation state for uranium is the hexavalent state for which the dominant species is the uranyl ion, UO_2^{2+}.[1−3] The redox chemistry of uranyl has been extensively investigated and manipulated, particularly for separations and process chemistry relating to the nuclear fuel cycle and other defense-related applications. However, there has been recent renewed interest in the redox behavior of uranium species (and related redox photochemical behavior) in relation to environmental fate and transport and mixed-waste treatment issues. Specifically, researchers are actively investigating ways to take advantage of the vast differences in aqueous solubility between the more soluble UO_2^{2+} species and highly insoluble U(IV) species to immobilize uranium thereby preventing migration of uranium contaminant plumes into aquifers and other groundwater resources. Approaches to driving this reduction process include using metal-reducing microbial organisms,[4−10] natural mineral surfaces,[11−14] and/or photochemical processes.[15−18]

One very important consideration in harnessing these environmentally inspired mechanisms to bring about UO_2^{2+} reduction is that the reducing agents have sufficient capability

[†] E-mail: demorris@lanl.gov.

(1) Weigel, F. *Uranium*, 2nd ed.; Katz, J. J., Seaborg, G. T., Morss, L. R., Eds.; Chapman & Hall: New York, 1986; Vol. 1, pp 169−442.
(2) Franz, C.; Schmitt, R. E. *Electrochemical Properties of Uranium in Solution*; Gmelin, L., Ed.; Springer−Verlag: Berlin, 1975; Vol. D1, pp 36−78.
(3) Martinot, L.; Fuger, J. *The Actinides*; Bard, A. J., Parsons, R., Jordan, J., Eds.; Marcel Dekker: New York, 1987; pp 631−673.
(4) Lojou, E.; Bianco, P. *J. Electroanal. Chem.* **1999**, *471*, 96−104.
(5) Tucker, M. D.; Barton, L. L.; Thomson, B. M. *Appl. Microbiol. Biotechnol.* **1996**, *46*, 74−77.
(6) Tebo, B. M.; Obraztsova, A. Y. *FEMS Microbiol. Lett.* **1998**, *162*, 193−198.
(7) Truex, M. J.; Peyton, B. M.; Valentine, N. B.; Gorby, Y. A. *Biotechnol. Bioeng.* **1997**, *55*, 490−496.
(8) Spear, J. R.; Figueroa, L. A.; Honeyman, B. D. *Environ. Sci. Technol.* **1999**, *33*, 2667−2675.
(9) Spear, J. R.; Figueroa, L. A.; Honeyman, B. D. *Appl. Environ. Microbiol.* **2000**, *66*, 3711−3721.
(10) Tsezos, M.; Georgousis, Z.; Remoudaki, E. *Biotechnol. Bioengin.* **1997**, *55*, 16−27.
(11) Wersin, P.; Hochella, M. F.; Persson, P.; Redden, G.; Leckie, J. O.; Harris, D. W. *Geochim. Cosmochim. Acta* **1994**, *58*, 2829−2843.
(12) Liger, E.; Charlet, L.; VanCappellen, P. *Geochim. Cosmochim. Acta* **1999**, *63*, 2939−2955.
(13) Charlet, L.; Silvester, E.; Liger, E. *Chem. Geol.* **1998**, *151*, 85−93.
(14) Baranger, P.; Disnar, J. R. *Bull. Soc. Geol. Fr.* **1991**, *162*, 271−276.
(15) McCleskey, T. M.; Foreman, T. M.; Hallman, E. E.; Burns, C. J.; Sauer, N. N. *Environ. Sci. Technol.* **2001**, *35*, 547−551.
(16) Wang, W. D.; Bakac, A.; Espenson, J. H. *Inorg. Chem.* **1995**, *34*, 6034−6039.
(17) Sarakha, M.; Bolte, M.; Burrows, H. D. *J. Photochem. Photobiol., A* **1997**, *107*, 101−106.
(18) Eliet, V.; Bidoglio, G. *Environ. Sci. Technol.* **1998**, *32*, 3155−3161.

10.1021/ic0201708 CCC: $22.00
Published on Web 05/31/2002

(both thermodynamic and kinetic) to effect the desired reduction process. The variability in redox energetics and kinetics for UO_2^{2+} species as a function of changes in the coordination environment in the equatorial plane about this *trans*-dioxo cation are frequently overlooked in researching and designing natural systems. In this report we examine the redox properties of a series of UO_2^{2+} coordination complexes as studied by cyclic voltammetry with particular attention to changes in the redox potentials and the heterogeneous electron-transfer kinetic parameters for the UO_2^{2+}/UO_2^{+} couple as a function of changes in the coordination environment.

Perhaps the most familiar feature of uranyl redox chemistry is the propensity of the one-electron-reduced species (UO_2^{+}) to undergo a rapid disproportionation reaction under a variety of conditions but particularly in acidic aqueous solution.[1,2,19] There are a number of equatorially coordinated ligands that have been found to provide at least limited stabilization of the pentavalent uranyl species (and thus simplified voltammetric behavior for to the UO_2^{2+}/UO_2^{+} couple). Voltammetric studies of the redox processes for some of these complexes have been reported.[20−26] Some coordination environments, such as provided by carbonate complexation, even provide sufficient stabilization of the pentavalent species to enable spectroscopic studies.[20,23,24] While there have been several reports and reviews of homogeneous electron-transfer kinetics for uranyl complexes,[19,27] much less attention has been devoted to investigating variations in the heterogeneous electron-transfer kinetic properties of this couple as a function of coordination environment. However, the voltammetric data have in many cases exhibited signs of electron-transfer-limited behavior instead of diffusion-limited behavior.[2,20,24,28,29] Ideally, significant benefit will be gained in the design and manipulation of redox-based remediation schemes if the role of UO_2^{2+} coordination environment on both the redox potential and the electron-transfer kinetics is better delineated and understood.

Experimental Section

Materials. All sample solutions (Table 1) were prepared from reagent grade materials used without additional purification. Uranyl nitrate hexahydrate [$UO_2(NO_3)_2{\cdot}6H_2O$] was obtained from Strem Chemicals. The appropriate uranyl complexes were prepared in situ using salts of the desired ligands: LiCl (Fisher Scientific); Na_2CO_3 (J. T. Baker); $Na(C_2H_3O_2)$ (J. T. Baker); $[(CH_3)_4N]OH$ (Aldrich). Sodium nitrate was used as a supporting electrolyte in some solutions as described below. Solution pH values were adjusted using 0.1 or 0.01 M solutions of either HNO_3 or NaOH. Solution pH values were measured using a Ross combination pH electrode (Orion model 8103) and an Orion model 290A pH meter. All solutions were freshly prepared and degassed with dry nitrogen for 15 min prior to acquisition of electrochemical data.

Table 1. Solution Compositions for Electrochemical Studies

ligand system	soln composn	$[UO_2^{2+}]_{tot}$ (mM)	pH	dominant uranyl species
aquo	1 M $NaNO_3$	10.0	3.0	$[UO_2(OH_2)_5]^{2+}$
hydroxo	2.0 M $[(CH_3)_4N]OH$[a]	11.4	n/a	$[UO_2(OH)_5]^{3-}$
acetato	1.0 M $Na(C_2H_3O_2)$[b]	2.0	5.9	$[UO_2(C_2H_3O_2)_3]^{-}$
carbonato	0.1 M Na_2CO_3[b]	2.2	11.3	$[UO_2(CO_3)_3]^{4-}$
chloro	12.3 M LiCl	11.1	2.4	$[UO_2Cl_4]^{2-}$

[a] This quarternary ammonium salt was required to prevent the formation of insoluble uranate salts. See ref 37. [b] These solutions also contained 0.1 M $NaNO_3$. These samples were part of a larger investigation of the electrochemistry at varying ligand concentrations, and the $NaNO_3$ was maintained at 0.1 M in these studies to serve as the background electrolyte.

Instrumentation. Electrochemical data were obtained with a Perkin-Elmer Princeton Applied Research Corporation (PARC) Model 263 Potentiostat under computer control using PARC model 270 software. For all complexes except $[UO_2Cl_4]^{2-}$ the data were obtained using a PARC model 303A static mercury drop electrode system with a hanging mercury drop for the working electrode. In these cases a fresh drop was used for each experimental cycle. For the uranyl chloride complex the potential region of electroactivity for the complex was too positive to enable use of a Hg working electrode. Thus, for this complex solution a PARC model K0264 microcell with an ~3 mm diameter Pt disk working electrode was used. A silver/silver chloride reference electrode and a Pt wire counter electrode were used in all experiments. Uncompensated resistance between the working and reference electrodes was measured for all solutions and found to be negligible except for the $[(CH_3)_4N]OH$ solution for which it was 150 Ω. For this solution the positive feedback *IR* compensation feature of the potentiostat/software was used.

Analyses and Simulations. The diffusion coefficients for both the oxidized and reduced forms of the uranyl complexes were determined for most complexes from fitting of double-potential step chronoamperometric data obtained with potential steps of sufficient magnitude to ensure that electron transfer was governed by diffusion control. Under these conditions the Cottrell equation was assumed to apply.[30] Thus, the diffusion coefficients were extracted from the slopes of the linear fit of measured current versus $(\text{time})^{-1/2}$ for the oxidized form from the cathodic current and the reduced form from the anodic current. For the aquo uranyl complex no chronoamperometric data were collected. Here the diffusion coefficient for the oxidized form of the complex was determined from cyclic voltammetric data by fitting of the peak current versus $(\text{scan rate})^{1/2}$ according to established formulas,[30] and the diffusion coefficient for the reduced form was assumed to be the same. Corrections for spherical electrodes were used in all these calculations. These diffusion coefficients are summarized in Table 2 and were explicitly input into the digital simulation software (see below) to obtain true electron-transfer rate constants.

(19) Newton, T. W. *The Kinetics of the Oxidation−Reduction Reactions of Uranium, Neptunium, Plutonium, and Americium in Aqueous Solutions*; NTIX: Springfield, VA, 1975.
(20) Wester, D. W.; Sullivan, J. C. *Inorg. Chem.* **1980**, *19*, 2838−2840.
(21) Jung, K.-S.; Sohn, S. C.; Ha, Y. K.; Eom, T. Y. *J. Electroanal. Chem.* **1991**, *315*, 113−124.
(22) Mizuguchi, K.; Lee, S. H.; Ikeda, Y.; Tomiyasu, H. *J. Alloys Compd.* **1998**, *271*, 163−167.
(23) Mizuguchi, K.; Park, Y. Y.; Tomiyasu, H.; Ikeda, Y. *J. Nucl. Sci. Technol.* **1993**, *30*, 542−548.
(24) Docrat, T. I.; Mosselmans, J. F. W.; Charnock, J. M.; Whiteley, M. W.; Collison, D.; Livens, F. R.; Jones, C.; Edmiston, M. J. *Inorg. Chem.* **1999**, *38*, 1879−1882.
(25) Lee, S. H.; Mizuguchi, K.; Tomiyasu, H.; Ikeda, Y. *J. Nucl. Sci. Technol.* **1996**, *33*, 190−192.
(26) Kim, S. Y.; Harada, M.; Tomiyasu, H.; Shiokawa, Y.; Ikeda, Y. *J. Nucl. Sci. Technol.* **2000**, *37*, 999−1002.
(27) Nash, K. L.; Sullivan, J. C. *Kinetics and Mechanisms of Actinide Redox and Complexation Reactions*; Sykes, A. G., Ed.; Academic Press: New York, 1986; Vol. 5, pp 185−213.
(28) Casadio, S.; Orlandini, F. *J. Electroanal. Chem.* **1970**, *26*, 91−96.
(29) Kim, K. W.; Kim, J. D.; Aoyagi, H.; Yoshida, Z. *J. Nucl. Sci. Technol.* **1994**, *31*, 329−334.
(30) Bard, A. J.; Faulkner, L. R. *Electrochemical Methods: Fundamentals and Applications*, 2nd ed.; John Wiley & Sons: New York, 2001.

Table 2. Redox Parameters for the UO_2^{2+}/UO_2^{+} Couples from Electrochemical Analyses

system	$10^6 D_{ox}$[a] (cm^2/s)	$10^6 D_{red}$[a] (cm^2/s)	k^0 (cm/s)	α	$E_{1/2}$ (V vs Ag/AgCl)
$[UO_2(C_2H_3O_2)_3]^{-/2-}$	6.0	5.3	>0.1[b]	~0.5[b]	−0.396
$[UO_2Cl_4]^{2-/3-}$	2.0	1.3	9.2×10^{-3}	0.30	−0.065
$[UO_2(OH_2)_5]^{2+/+}$	0.7[c]	0.7[c]	9.0×10^{-3}	0.50	−0.169
$[UO_2(OH)_5]^{3-/4-}$	4.3	3.4	2.8×10^{-3}	0.46	−0.927
$[UO_2(CO_3)_3]^{4-/5-}$	7.2	6.3	2.6×10^{-5}	0.41	−0.820

[a] Diffusion coefficients determined from fits to double-potential step chronoamperometric data; D_{ox} is the coefficient for the oxidized species, and D_{red} that for the reduced species. [b] Electron transfer for this system is diffusion limited; kinetic parameters cannot be extracted from simulations, but estimates are provided. See text for details. [c] D_{ox} determined from cyclic voltammetric data; D_{red} assumed to be equal to D_{ox}.

All raw electrochemical data were analyzed using the software package IGOR Pro (v. 4.1) from WaveMetrics, Inc., operating on an Apple Macintosh platform. The peak potentials and currents for the voltammetric peaks were determined by fitting the region about the peak location using a fourth-order polynomial and solving for the extremum. The raw chronoamperometric data were converted to a linearized form (i versus $t^{-1/2}$) and fit using a linear least-squares routine. The heterogeneous electron-transfer kinetic parameters, including the rate constant, k^0, and the electron-transfer coefficient, α, were determined by digital simulations of the cyclic voltammetric data as a function of the scan rate. The digital simulation is based on the method of finite differences.[31] The simulator, written in Fortran and running on a Macintosh platform, generates simulated voltammograms over a specified range of scan rates from which three metrical parameters are extracted at each discrete scan rate for comparison with the actual experimental data: the cathodic peak potential (E_{pc}); the difference between the cathodic and anodic peak potentials ($\Delta E_p = E_{pc} - E_{pa}$); the cathodic potential at half of the maximum cathodic peak current ($E_{pc/2}$). The best fit of the simulated data to the experimental data was determined iteratively by varying the values of $E_{1/2}$, k^0, and α in the simulator. The sensitivity of the quality of this fit to variations in parameters is illustrated below. The dependence of the metrical parameters on these three intrinsic system constants is convoluted. However, from a phenomenological standpoint, E_{pc} is most dependent on $E_{1/2}$, ΔE_p is most dependent on k^0, and $E_{pc/2}$ is most dependent on α. This approach has been described previously by us to determine the heterogeneous electron-transfer kinetic constants for the Bk(IV/III) couple in carbonate media.[32]

Results and Discussion

A number of factors entered into the selection of the uranyl coordination complexes for investigation in this report. First was the desire to focus specifically on (1) variations in redox energetics for the UO_2^{2+}/UO_2^{+} couple and (2) determination of the heterogeneous electron-transfer kinetics for this couple as a function of different coordination environments. This latter issue in particular mandated significant constraints on the ultimate systems, because variations in solution compositions (ligand-to-metal concentration ratios and/or pH) for any of these uranyl/complexing ligand mixtures can lead to chemical complications coupled to the reduction process. These complications can vary from disproportionation of UO_2^{+} species as noted above to simple protonation equilibria for the complexed ligands in conjunction with the redox transformation as seen, for example, in the uranyl−ethylenediaminetetraacetic acid (EDTA) system.[33] Such complications preclude a simple analysis of the voltammetric data to extract the kinetic information and were, therefore, avoided.

Another factor guiding the selection process was the desire to retain a high degree of symmetry in the equatorial coordination sphere to simplify consideration of the changes in the molecular structure between the oxidized and reduced forms of the complexes (see discussion below). Thus, the focus was on the limiting (i.e., fully ligated) forms of the coordination complexes instead of mixed-ligand complexes (e.g., partially aquated or hydroxylated species) that are prevalent in these systems at low ligand-to-metal concentration ratios. Not surprisingly, the simplest voltammetric behavior was typically observed under conditions favoring these limiting complexes. The speciation under these conditions (the metal−ligand stoichiometry in particular) for the aquo, acetate, and carbonate ligand systems has been described and assigned previously in the literature on the basis of potentiometric and/or spectroscopic evidence.[20,23,24,34−40] The speciation for the uranyl chloride system is inferred from similar work on the neptunyl and plutonyl chloride systems[41,42] and unpublished data on the uranyl system.[43] The speciation for the hydroxide complex is based on our own recent work and other published data.[37,40,44] Thus, there is confidence that the voltammetric data were obtained in all cases for nearly pure single-species solutions of uranyl complexes having fully ligated equatorial planes containing only the target ligands.

Finally, we also concentrated on systems that have some environmental and/or waste treatment significance. This was done in support of the original premise that an understanding and accounting of the redox properties for these systems is crucial to the successful design of natural remediation systems. The aquo, carbonato, acetato, and chloro complexes of uranyl are all known or potentially relevant species in environmental groundwaters, and the hydroxo and carbonato complexes are relevant species in alkaline high-level radioactive waste storage tanks associated with nuclear fuel process-

(31) Feldberg, S. W. *Electrochemistry*; Mattson, J. S., Mark, J. H. B., MacDonald, J. H. C., Eds.; Marcel Dekker: New York, 1972; Vol. 2, Chapter 7.
(32) Morris, D. E.; Hobart, D. E.; Palmer, P. D.; Haire, R. G.; Peterson, J. R. *Radiochim. Acta* **1990**, *49*, 125−134.
(33) Baker, B. C.; Sawyer, D. T. *Inorg. Chem.* **1970**, *9*, 197.
(34) Allen, P. G.; Bucher, J. J.; Clark, D. L.; Edelstein, N. M.; Ekberg, S. A.; Gohdes, J. W.; Hudson, E. A.; Kaltsoyannis, N.; Lukens, W. W.; Neu, M. P.; Palmer, P. D.; Reich, T.; Shuh, D. K.; Tait, C. D.; Zwick, B. D. *Inorg. Chem.* **1995**, *34*, 4797−4807.
(35) Clark, D. L.; Hobart, D. E.; Neu, M. P. *Chem. Rev.* **1995**, *95*, 25−48.
(36) Quiles, F.; Burneau, A. *Vib. Spectrosc.* **1998**, *18*, 61−75.
(37) Clark, D. L.; Conradson, S. D.; Donohoe, R. J.; Keogh, D. W.; Morris, D. E.; Palmer, P. D.; Rogers, R. D.; Tait, C. D. *Inorg. Chem.* **1999**, *38*, 1456−1466.
(38) Grenthe, I. *The Chemical Thermodynamics of Uranium*; North-Holland: New York, 1992.
(39) Quiles, F.; Burneau, A. *Vib. Spectrosc.* **2000**, *23*, 231−241.
(40) Moulin, C.; Decambox, P.; Moulin, V.; Decaillon, J. G. *Anal. Chem.* **1995**, *67*, 348−353.
(41) Runde, W.; Neu, M. P.; Clark, D. L. *Geochim. Cosmochim. Acta* **1996**, *60*, 2065−2073.
(42) Runde, W.; Reilly, S. D.; Neu, M. P. *Geochim. Cosmochim. Acta* **1999**, *63*, 3443−3449.
(43) Runde, W. Personal communication of unpublished results.
(44) Moll, H.; Reich, T.; Szabo, Z. *Radiochim. Acta* **2000**, *88*, 411−415.

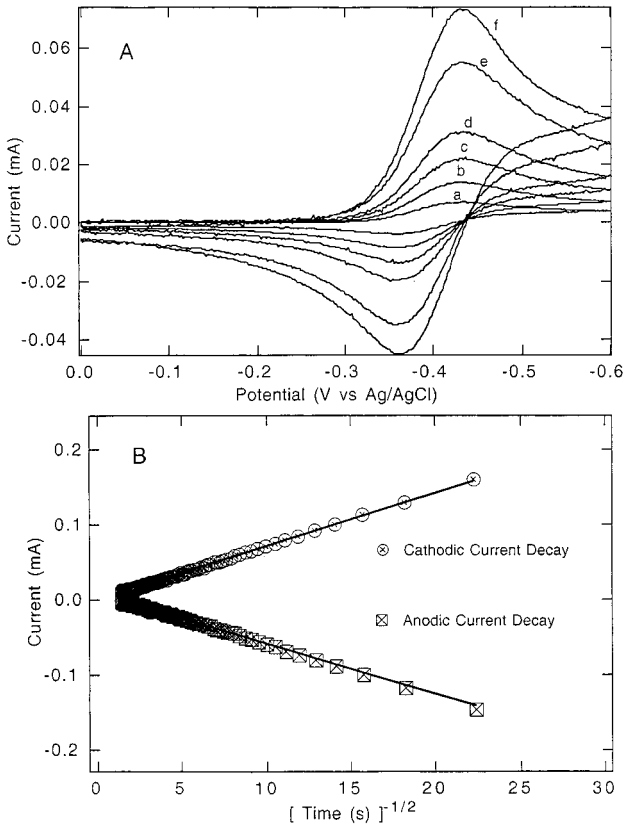

Figure 1. Electrochemical data for 2 mM UO_2^{2+} in 1.0 M $Na(C_2H_3O_2)$/0.1 M $NaNO_3$ at pH 5.9 at a Hg electrode: (A) cyclic voltammograms at (a) 50, (b) 200, (c) 500, (d) 1000, (e) 3000, and (f) 5000 mV/s scan rate; (B) linearized double-potential step chronoamperometric data for a cathodic potential step from 0.0 to −0.7 V (vs Ag/AgCl) and an anodic potential step from −0.7 V to 0.0 V. The reversal time was 0.5 s, and anodic decay data have been corrected for this offset time. Straight lines are the linear least-squares fits to all data points.

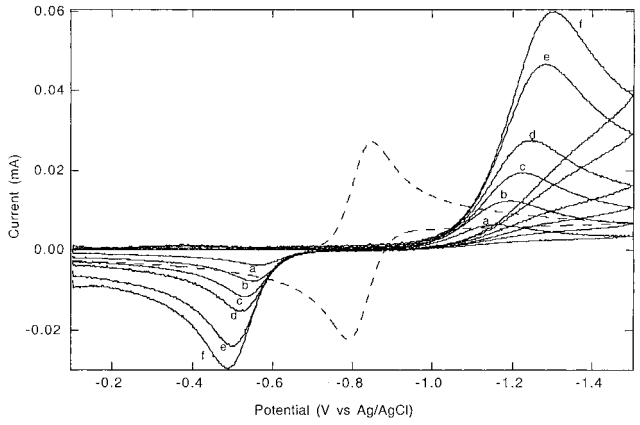

Figure 2. Cyclic voltammograms for 2.2 mM UO_2^{2+} in 0.1 M Na_2CO_3/0.1 M $NaNO_3$ at pH 11.3 at a Hg electrode at scan rates of (a) 50, (b) 200, (c) 500, (d) 1000, (e) 3000, and (f) 5000 mV/s. The dashed line is a simulated voltammogram for a system having the same $E_{1/2}$ value but with diffusion-limited electron-transfer behavior ($k^0 = 1$ cm/s) and $\alpha = 0.5$. See text for details.

ing. The ultimate optimal system compositions are summarized in Table 1.

Typical electrochemical data spanning the range of electron-transfer kinetic behavior are illustrated in Figures 1 and 2. The uranyl/acetate system exhibits nearly ideal diffusion-limited heterogeneous electron-transfer behavior as shown in the cyclic voltammograms in Figure 1A. The separation between the cathodic and anodic peaks in this system is essentially independent of scan rate over the range from 20 to 5000 mV/s. The average value determined from 14 scan rates is 73.1 ± 0.4 mV. This value is in agreement with the theoretical value (59 mV) for a reversible one-electron couple.[30] Because this redox couple does fall within the diffusion-limited electron-transfer kinetic regime for the accessible scan-rate range, it was not possible to use the digital simulation approach to determine the electron-transfer kinetic parameters. However, the rate constant must be at least 0.1 cm/s for the ΔE_p value to be independent of scan rate over the range investigated.

Figure 1B is illustrative of the general behavior observed for all these uranyl complexes in the double-potential step chronoamperometric experiments. Both the cathodic current resulting from the step to reducing potentials (−0.7 V vs Ag/AgCl in the present case) and the anodic current from the reverse potential step to oxidizing conditions (0.0 V in this case) show ideal time$^{-1/2}$ decay behavior indicative of being within the diffusion-limited electron-transfer kinetic regime. The linear fits to these data (Figure 1B for the acetate system) are quite good for all the complexes. The slopes of these fits were used to determine the diffusion coefficients according to the Cottrell equation, the cathodic current decay providing the diffusion coefficient for the oxidized form (D_{ox}) and the anodic current decay providing the coefficient for the reduced form (D_{red}). These results for all the uranyl complexes are summarized in Table 2.

In contrast to the behavior of the uranyl acetate system (Figure 1A), the cyclic voltammetry of the uranyl carbonate system falls clearly within the regime of electron-transfer limited kinetic behavior (Figure 2). For comparison, a simulated voltammogram of an ideal reversible redox couple is provided. Note that there is an enormous dependence of the separation between the cathodic and anodic peaks on the scan rate. The ΔE_p value ranges from 570 mV at 20 mV/s to 810 mV at 5000 mV/s. Note, too, that there is a marked asymmetry between the cathodic and anodic peaks indicating that the barriers to electron transfer differ in the forward and reverse directions (i.e., $\alpha \neq 0.5$). The voltammetric data for the other three uranyl complexes (Table 1) fall between that illustrated for the acetate and carbonate complexes. The data for the carbonate complex and these other three are readily amenable to electron-transfer kinetic analysis by the digital simulation method.

The digital simulations were performed for all systems but the acetate complex using best initial guesses for $E_{1/2}$, k^0, and α and iterating to the best fit of the experimental voltammetric parameters, E_{pc}, ΔE_p, and $E_{pc/2}$. The results are summarized in Table 2. A graphical illustration of the outcome of this simulation/fitting procedure is provided in Figure 3 for the uranyl carbonate system. The quality of the best fit (solid lines in Figure 3) is quite good over the entire scan rate range. Comparable fits were achieved for the aquo, hydroxo, and chloro complexes. Figure 3 also illustrates the sensitivity of the quality of this best fit to small variations (±10%) in the best fit parameter values for k^0 (Figure 3A)

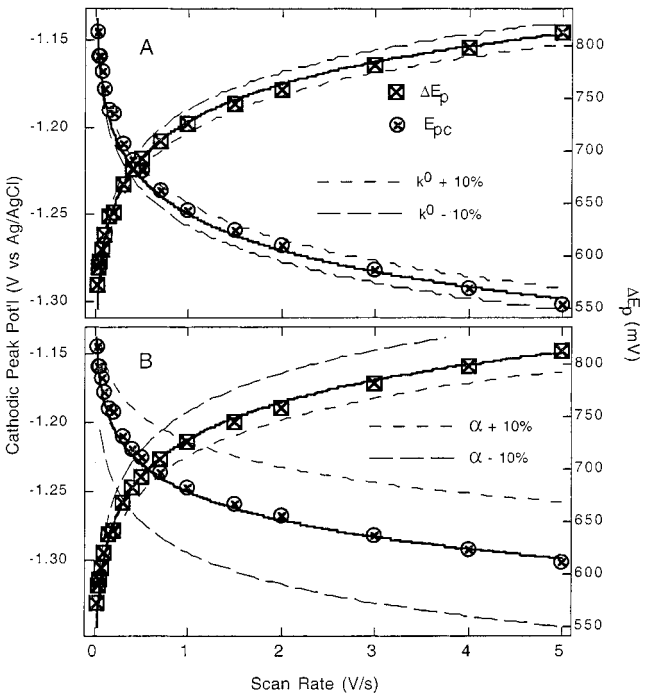

Figure 3. Results of digital simulations of cyclic voltammetric data as a function of scan rate for 2.2 mM UO_2^{2+} in 0.1 M Na_2CO_3/0.1 M $NaNO_3$ at pH 11.3 at a Hg electrode illustrating the best fit to the data from iterative variations in $E_{1/2}$, k^0, and α and the sensitivity of the best fit to variations in these parameters. The solid line is for the best fit values for all parameters (see Table 2). Key: (A) sensitivity of fit to variations in k^0 keeping $E_{1/2}$ and α at best-fit values; (B) sensitivity of fit to variations in α keeping $E_{1/2}$ and k^0 at best-fit values.

and α (Figure 3B). This provides some semiquantitative estimate of the uncertainty in the kinetic parameters provided in Table 2. The uncertainties are clearly much better than 10% in all cases. Note that, for given values of k^0 and α, variations in the simulation for $E_{1/2}$ result in a constant offset in the simulated E_{pc} and $E_{pc/2}$ values over the entire scan-rate range. Thus, the simulated $E_{1/2}$ value was adjusted last in the process to bring the best-fit line into coincidence with the experimental data. Variations in the $E_{1/2}$ values of ±5 mV from the best-fit values very noticeably degraded the quality of fits in all cases. This provides some measure of the uncertainty in this best-fit parameter value.

The range of $E_{1/2}$ values spanned by the complexes investigated in this report (Table 2) is very nearly 1 V and chiefly reflects the large differences in the *σ*-donor ability of the ligands and the impact this has on the energy of the lowest unoccupied molecular orbital (of mostly 5f orbital parentage) in the uranyl moiety. This variability vividly illustrates the importance of explicitly considering the probable speciation of the uranium in the design and manipulation of redox-based remediation processes. The results for the aquo complex versus the carbonate complex are of particular significance with respect to groundwater contamination by uranium. The tris(carbonato) complex is widely regarded as the most probable soluble form of uranium in aerobic, surface, and near-surface waters,[35,38] yet the aquo complex of uranyl and its hydrolysis products appear to be the ones most commonly considered in environmental fate and transport studies. There are likely to be many reducing agents capable of reducing the aquo complex, but there are likely far fewer naturally occurring redox agents capable of reducing the tris(carbonato) complex.

The range of values in the electron-transfer rate constant as a function of equatorial coordination environment (Table 2) is also quite large, although the specific molecular origin of this effect is much less readily ascribable than is the variability in $E_{1/2}$ with coordination environment. Interpretations of the fundamental aspects of heterogeneous electron transfer processes are typically based on Marcus theory of electron transfer in homogeneous systems (see ref 30 and references therein). In this Marcus description, slow electron-transfer kinetics are typically associated with large structural rearrangements accompanying the electron-transfer step. Other "outer-sphere" effects can contribute to slow electron transfer including large work terms associated with bringing the reactants to the equilibrium electron-transfer configuration at the electrode surface and/or solvent reorganizational effects. However, there are no readily discernible trends in the variations in k^0 for these uranyl complexes with the charge on the reactants or products or the solvent/supporting electrolyte composition that would suggest that these other factors are principally responsible for the observed rate constants. For example, the tetrachloro, aquo, and hydroxo complexes have similar rate constants (Table 2) but markedly different charges on the complex ions and substantially different electrolyte compositions.

If, in fact, the origin of the slow kinetics lies principally with a large structural rearrangement accompanying the electron transfer, then comparison of the structural data for the uranyl species in the hexavalent versus pentavalent state should provide some insight. As noted above, pentavalent uranyl species are notoriously unstable with respect to disproportionation, so there are very limited structural characterization data for UO_2^+ species. However, there have been recent reports on the X-ray absorption spectroscopic characterization[24] and computational structural optimization[45] of the uranyl tris(carbonate) complex in both the oxidized and reduced form. Experimentally, the axial U═O bond length increases by 0.10 Å and the average $U-O_{carbonate}$ equatorial bond length increases by 0.07 Å on reduction of the metal center. Results from the computational study generally mimic these experimental observations. The computational effort also considered torsional distortions of the bidentate coordinated carbonate ligands from D_{3h} to C_3 symmetry in association with the reduction process, but the resulting distorted pentavalent uranyl species was found to be less stable than the planar (D_{3h}) reduced species. Thus, both theory and experiment suggest that the structural changes that occur upon reduction are elongations in the metal-"yl"−oxygen and metal−equatorial oxygen bond lengths as anticipated.

Comparable experimental or theoretical data are not available for the other uranyl coordination complexes investigated in the present report. However, similar X-ray

(45) Gagliardi, L.; Grenthe, I.; Roos, B. O. *Inorg. Chem.* **2001**, *40*, 2976−2978.

absorption data have been collected for the corresponding neptunyl tris(carbonate) complex in both oxidation states (i.e., NpO_2^{2+} and NpO_2^{+}).[46,47] On the basis of published reports of the cyclic voltammetry of this neptunium system,[48] the electron-transfer rate constant is substantially greater than in the corresponding uranyl carbonate system. For the neptunyl carbonate complex the axial Np═O bond length increases by 0.09 Å and the average $Np-O_{carbonate}$ equatorial bond length increases by 0.09 Å on reduction of the metal center. These data alone do not lead to any strong conclusions regarding a cause-and-effect relationship between structural distortion and electron-transfer rate. However, there does appear to be a greater delocalization of the distortion over all the metal−oxygen bonds for neptunyl than for uranyl on changing the oxidation state, suggesting that a faster electron-transfer rate might be facilitated by spreading the reorganization over many bonds.

The structure of the optical excited state in these UO_2^{2+} complex systems should also be a reasonable approximation of that of the electrochemically reduced species (UO_2^{+}), since the optical excitation in these systems entails the promotion of an essentially nonbonding electron on the axial oxo atom(s) to the lowest unoccupied orbital on the metal center. This terminal optical orbital should be the same as the redox orbital in the one-electron reduction. The structural distortion between the ground state and the optical excited state should then be a facsimile of that in the redox process. The emission spectrum for these uranyl complexes provides an indirect measure of the distortion in the axial U═O bond length between the ground and excited states through the intensity pattern in the vibronically resolved spectrum. This occurs because the intensity pattern is determined by the extent of structural distortion in the U═O bonds reflected by the magnitude of the Franck−Condon factor. However, comparison of the vibronic intensity pattern for all of these complexes shows that it is essentially the same in each suggesting that the distortion in the U═O bond length is comparable in each. Thus, if a large structural distortion is the origin of the slow electron-transfer kinetics, the key element(s) of the distortion must encompass molecular coordinates besides, or at least in addition to, the U═O bonds.

The recent theoretical results of Gagliardi et al.[45] are promising in that they demonstrate that reliable calculations of structural changes accompanying the one-electron reduction of uranyl complexes can be made. Thus, it may be possible to assess such structural changes in complexes that do not show sluggish electron-transfer kinetics (e.g., the tris(acetato) complex). Comparisons to systems that do show slow kinetics (e.g., the tris(carbonato) complex) may make it possible to pinpoint any structural origin for this effect. Regardless of the origin of the sluggishness of electron transfer in some of these uranyl complexes, the significance cannot be overlooked. The general consequence of slow electron-transfer kinetics is to further exacerbate the difficulty in reducing the complex because of the added activation barrier (the redox overpotential) to reduction. Even in homogeneous electron-transfer reactions between uranyl and a soluble reducing agent there may be similar obligatory structural rearrangements required in the uranyl complex that will inhibit the overall efficiency of the electron-transfer process,[27] potentially disabling the homogeneous reduction process and shutting down the remediation scheme.

Acknowledgment. This research was performed at Los Alamos National Laboratory under contract with the University of California (Contract No. W-7405-ENG-36) with support from the United States Department of Energy, Offices of Science and Environmental Management, under the auspices of the Environmental Management Science Program and Los Alamos National Laboratory's Laboratory Directed Research and Development program. The author is grateful to Drs. David L. Clark and Wolfgang Runde of Los Alamos for helpful discussions relating to the preparation of the uranyl carbonate and chloride complexes, respectively. The author also acknowledges Drs. D. Webster Keogh and Robert J. Donohoe of Los Alamos for their thorough review and comments on the manuscript.

IC0201708

(46) Tait, C. D. Personal communication of unpublished results.
(47) Clark, D. L.; Conradson, S. D.; Ekberg, S. A.; Hess, N. J.; Neu, M. P.; Palmer, P. D.; Runde, W.; Tait, C. D. *J. Am. Chem. Soc.* **1996**, *118*, 2089−2090.
(48) Varlashkin, P. G.; Hobart, D. E.; Begun, G. M.; Peterson, J. R. *Radiochim. Acta* **1984**, *35*, 91−96.